JOURNAL OF MAGNETIC RESONANCE **131,** 248–253 (1998)
ARTICLE NO. MN981365

An NMR Investigation of the Conformational Effect of Nitroxide Spin Labels on Ala-Rich Helical Peptides

Kimberly A. Bolin, Paul Hanson, Sarah J. Wright, and Glenn L. Millhauser[1]

Department of Chemistry and Biochemistry, University of California, Santa Cruz, California 95064

Received June 26, 1997; revised November 6, 1997

Nitroxide spin labels, in conjunction with electron spin resonance (ESR) experiments, are extensively employed to probe the structure and dynamics of biomolecules. One of the most ubiquitous spin labeling reagents is the methanethiosulfonate spin label which attaches a spin label selectively to Cys residues via a disulfide bond (Cys-SL). However, the actual effect of the nitroxide spin label upon the conformation of the peptide or protein cannot be unambiguously determined by ESR. In this study, a series of 16-residue Ala-rich helical peptides was characterized by nuclear magnetic resonance techniques. The $C_\alpha H$ chemical shift analysis, NOEs, and $^3J_{NH\alpha}$ coupling constants for peptides with no Cys, free Cys, and Cys-SL (with the N–O group reduced) were compared. These results indicate that while replacement of an Ala with a Cys residue causes a loss of overall helical structure, the Cys-SL residue is helix supporting, as would be expected for a non-β-branched aliphatic amino acid. Thus, the Cys-SL residue does not perturb helical structure and, instead, exhibits helix-stabilizing characteristics similar to that found for Ala, Met, and Leu.

INTRODUCTION

The use of electron spin resonance (ESR)[2] and selective spin labeling for the measurement of distances and the elucidation of structure in biomolecules is an active and expanding field with methanethiosulfonate spin label (MTSSL), the most commonly used spin labeling reagent. MTSSL attaches a spin label directly to Cys forming an unbranched Cys-SL side chain (*1–3*). In addition to probing the nature of the equilibrium between α- and 3_{10}-helices in linear peptides (*4–6*), MTSSL has been used to probe a variety of systems, ranging from linear peptides (*7*) to integral membrane proteins (*8, 9*). Shin and co-workers recently developed a ''spectroscopic ruler'' for determining distances from 8 to 25 Å using the deconvolution of dipolar-coupled spectra of model Ala-rich α-helical peptides (*10*). This method should be applicable to numerous systems, including large or membrane-bound proteins. Other work on peptide systems by Cafiso and co-workers used ESR to determine the orientation and insertion depth of alamethicin, a voltage-gated channel forming peptide, with respect to the membrane surface (*7, 11*). ESR results from a series of peptides labeled with MTSSL at various positions parallel recent solid-state NMR results and confirm that alamethicin inserts with the helix axis normal to the lipid bilayer, the N-terminus completely buried within the membrane, and the C-terminus in the aqueous region approximately 4 Å from the membrane–solution interface (*7*). Some of the most extensive work utilizing MTSSL is being carried out by Hubbell and co-workers on a variety of systems, ranging from medium-sized proteins such as T4 lysozyme to membrane-bound proteins such as bacteriorhodopsin and lactose permease. For T4 lysozyme, Mchaourab *et al.* (*12*) were able to show that the hinge bending hinted at in crystal structures of the protein did in fact occur upon binding of the substrate. For both bacteriorhodopsin and lactose permease, a technique known as site-directed spin labeling (SDSL) was utilized (*8, 9*) where single Cys mutations are scanned through the sequence and then the mutants specifically labeled with MTSSL at the Cys. Using the periodic patterns built up from lineshape analysis and the influence of O_2 on the power saturation behavior of the ESR spectrum, both the mobility and the accessibility of various regions of the protein can be determined. α-helices are characterized by an obvious 3.6 residue periodicity and are easily identified as are loops and turns of greater mobility and accessibility. The breadth and extent of the applications of spin labeling to a variety of biological systems is only briefly touched upon here, but the importance and versatility of this technique are obvious.

In order to probe the conformational effect of the Cys-SL side-chain moiety, Hubbell and co-workers compared the

[1] To whom correspondence should be addressed. Fax: (408) 459-2935. E-mail: glennm@hydrogen.ucsc.edu.

[2] Abbreviations used: CD, circular dichroism; ESR, electron spin resonance; NMR, nuclear magnetic resonance; MRE, mean residue ellipticity; MTSSL, methanethiosulfonate spin label; Cys-SL, spin-labeled Cys residue; 3K8u, unlabeled 3K8 peptide; 3K8sl, N–O-reduced spin-labeled 3K8 peptide; 3K12u, unlabeled 3K12 peptide; 3K12sl, N–O-reduced spin-labeled 3K12 peptide; $^3J_{HN\alpha}$, three-bond αH–NH scalar coupling constant; conformational shift, experimental chemical shift − random coil chemical shift; NOE, nuclear Overhauser enhancement; NOESY, two-dimensional nuclear Overhauser spectroscopy; TOCSY, two-dimensional total correlation spectroscopy; NH–NH(i, j), NOE between NH of residue i and NH of residue j; αN(i, j), NOE between αH of residue i and NH of residue j; $\alpha\beta$(i, j), NOE between αH of residue i and βH of residue j; τ_M, mixing time.

1090-7807/98 $25.00

circular dichroism (CD) spectra, biological activity, and free energy of folding of 30 T4 lysozyme single Cys-SL mutants with the wild-type protein data (*13*). Of the numerous sites tested, only the most buried sites showed a loss of activity, similar to that observed for natural amino acid mutants. For sites in α-helices throughout the protein, there were no measured changes in stability or activity and CD did not detect any change in secondary structure between the wild-type and the Cys-SL mutants. Although extensive site-directed spin labeling work by Hubbell and co-workers in T4 lysozyme and other proteins suggests that the Cys-SL side chain does not significantly perturb secondary structure, these methods cannot probe local structural changes on a residue-specific basis. It is important to investigate the changes to the secondary structure that may be induced by the Cys-SL side chain. To address the conformational preferences of the Cys-SL side chain (see Fig. 1), a series of five peptides was investigated using NMR methods. These included 3K0 and two forms of 3K8 and 3K12: 3K8u (free Cys), 3K8sl (N–O-reduced Cys-SL), 3K12u (free Cys), and 3K12sl (N–O-reduced Cys-SL).

Ac-AAAAKAAAAKAAAAKA-NH_2 [3K0]

Ac-AAAAKAAC̲AKAAAAKA-NH_2 [3K8]

Ac-AAAAKAAAAKAC̲AAKA-NH_2 [3K12]

These peptides are variants on the 3K sequences first developed by Baldwin and co-workers and have been shown to be highly structured monomeric helices in aqueous solution (*14*). Further investigation of the peptides by ESR showed them to be a mixture of 3_{10}- and α-helical, with the α-helical structure predominating in the center of the peptide (*15*). While 3K0 cannot be studied by ESR, it is surprisingly amenable to study by NMR and shows an unanticipated degree of signal dispersion of the amide resonances (*16*). Measurement and analysis of the short-range NOEs, $^3J_{NH\alpha}$ coupling constants, and $C_\alpha H$ conformational shifts were readily accomplished for each of the three peptides and revealed characteristic values for helices: short-range NOEs, coupling constants less than 6 Hz, and upfield-shifted NH and $C_\alpha H$ chemical shifts. The data for the 3K0 peptide are compared to the data for both the free Cys (3K8u and 3K12u) and the N–O-reduced spin-labeled (3K8sl and 3K12sl) forms of the 3K8 and 3K12 peptides and investigated for evidence of conformational changes related to the substitution of the Cys or Cys-SL for an Ala residue. The NMR data suggest that the Cys-SL side chain does not perturb local helix structure when compared to the template/control peptide 3K0 and instead exhibits helix-supporting character similar to other unbranched aliphatic side chains.

MATERIALS AND METHODS

Peptide Synthesis and Purification

Peptides were synthesized by Fmoc solid-phase synthesis on a Rainin PS3 peptide synthesizer using a Rink amide resin. Purification and analysis were performed according to previously reported protocols (*4*).

Circular Dichroism

CD spectra were acquired on an Aviv 60DS spectropolarimeter, calibrated with (+)-10-camphorsulfonic acid, in 5 mM Mops buffer, at 1°C and pH 7.1. Peptide concentrations were in the range of 50–180 μM and samples contained at least 170 μL of sample in a 0.1-cm pathlength cuvette. Concentrations were determined by double integration of ESR spectra and comparison to a 1 mM 4-hydroxy-TEMPO standard solution. Peptide concentrations are accurate to 5%.

Nuclear Magnetic Resonance

All peptide samples were prepared as 3–4 mM peptide at pH 5.0 in 50 mM phosphate buffer containing 10% D_2O and azide. Sample pH was adjusted using 0.5 to 1.0 M solutions of HCl and NaOH. Sample volumes were 750 μL in a 5 mm NMR tube. Prior to NMR experiments, an aliquot of the final NMR sample was analyzed by HPLC monitored at 215 nm to ensure purity in excess of 95%.

^{1}H NMR experiments were performed on a Varian Unity Plus spectrometer with a ^{1}H frequency of 500 MHz using a 5 mm inverse detection probe, at 2°C. Temperature was calibrated using a methanol standard sample. Both TOCSY and NOESY experiments were routinely collected with a 6000 Hz spectral width, 4096 complex points in t_2, and 16 transients per t_1 increment. TOCSY spectra were acquired with 350 to 500 t_1 increments while τ_m = 400 ms NOESY spectra were acquired with between 800 and 1024 t_1 increments. TOCSY spectra were acquired with τ_m = 50 ms. Solvent saturation was applied for 1.5 s before the first 90° pulse and during the mixing time for NOESY spectra. TOCSY data were zero-filled to 1024 × 4096 and multiplied by a shifted (π/1.6 in t_2 and π/2.0 in t_1) sine-bell window before Fourier transformation. NOESY spectra were zero-filled to 2048 × 4096 and multiplied by a shifted (π/2.0) sine-bell window function. The NMR spectra were processed on a Silicon Graphics Indy using the MNMR package (Carlsberg Laboratory, Department of Chemistry, Denmark) and analyzed using XEASY (*17*). Chemical shifts were referenced to an internal standard of dioxane at 3.743 ppm. $^3J_{NH\alpha}$ coupling constants were measured using the INFIT module in XEASY according the method of Szyperski *et al.* (*18*).

Data reported for the 3K0 peptide were acquired under nearly identical conditions at the Nijmegen SON Research Center, University of Nijmegen, The Netherlands (*16*).

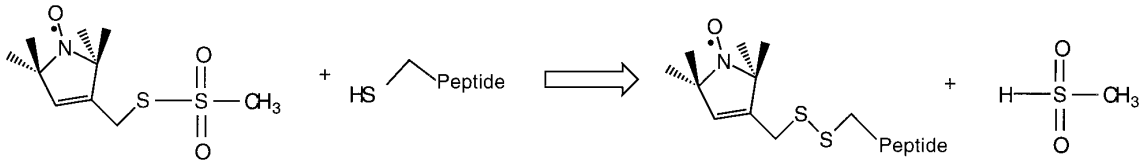

FIG. 1. MTSSL spin labeling reaction.

Preparation of N–O-Reduced Cys-SL Peptide NMR Samples

Cys-containing peptides were labeled with MTSSL according to previously reported procedures (*19*) using the scheme shown in Fig. 1 and further purified by reverse-phase HPLC as described above.

Lyophilized samples were dissolved in approximately 500 μL of phosphate buffer (10% D_2O) at pH 5. A solution of 0.2 M ascorbic acid was prepared using the phosphate buffer stock and titrated into the peptide solution in 5 to 20 μL aliquots. After each addition of ascorbic acid, the solution was left for approximately 30 min. A 40-μL sample was then extracted for ESR measurements using a Bruker ESP-380 running in CW mode. The ESR was equipped with a TE_{102} cavity and a Bruker temperature controller set to 300 K. Spectra were obtained with scanwidths of 80 G centered at 3357 G, and a modulation amplitude of 0.3 G. This process was continued until the peptide solution was ESR silent. The peptide solution was then brought to the NMR sample volume of 750 μL and the pH adjusted to pH 5.

RESULTS AND DISCUSSION

The CD spectra for 3K8sl and 3K12sl are nearly identical (Fig. 2), with the differences in MREs (mean residue ellipticity) similar to those reported for other 3K variants (*4*).

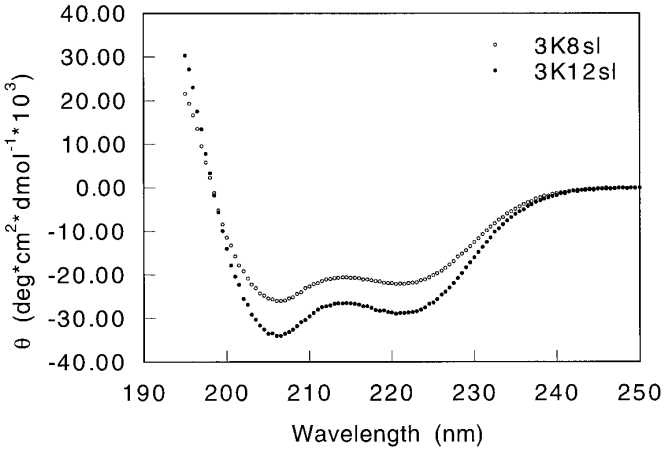

FIG. 2. CD spectra of 3K8sl and 3K12sl peptides in Mops buffer at pH 7.1 and 1°C. Both spin-labeled peptides exhibit spectra similar to the parent 3K0 peptide.

Despite the difference in absolute MREs for 3K12sl and 3K8sl, the ratio of the MREs at 222 nm vs 208 nm is the same, approximately 0.88. From previous work with spin-labeled peptides, there seems to be a position dependence to the CD signal; however, whether the effect is from the pseudo-chromorphic nature of the spin label interacting with the helix remains unclear (*20*). For 3K8u and 3K12u (data not shown), the ratios are 0.78 and 0.87, respectively, reflecting the relative increase in the negative minima at 208 nm and highlighting the helix-breaking effect of the Cys residue. The effect of the helix-breaking residue Cys at position 8 appears to be greater than that at position 12 for the 3K8u and 3K12u (unlabeled) peptides, but this is consistent with the position dependence previously observed for the stronger helix-breaking residue Gly (*21*).

The NMR spectra for the series of 3K peptides show amide resonances which are surprisingly well resolved for such homogeneous sequences. For 3K0, 13 of the 16 residues are immediately identifiable in the TOCSY spectrum, with the remaining three residues readily assigned using standard methods (*22*). The 3K8u, 3K8sl, 3K12u, and 3K12sl peptide spectra exhibit more signal overlap than the 3K0 spectra, but all backbone and greater than 90% of the side-chain protons were assigned for both the unlabeled and the Cys-SL versions. An example spectrum is shown in Fig. 3, the NH–NH region of the 3K12sl peptide. While there is good signal dispersion for the amide protons, the $C_\alpha H$ resonances are almost completely overlapped, as are the $C_\beta H$ resonances for the Ala residues. The high degree of overlap in these regions severely limits the use of medium-range NOEs, particularly the $\alpha N(i, i + 3)$, $\alpha N(i, i + 4)$, and $\alpha\beta(i, i + 3)$ NOEs, for characterizing the secondary structure of the peptide. However, a number of NH–NH $(i, i + 1)$ NOEs, shown in Fig. 3, and NH–NH $(i, i + 2)$ NOEs, characteristic of helical structure, can be readily identified for each of the peptides. While accidental overlap obscures some of the NH–NH NOEs, it is apparent from the NOE summary in Fig. 4 that the NOEs for 3K0 and the N–O-reduced Cys-SL peptides (3K8sl and 3K12sl) are consistent with a more helical conformation than is observed for the unlabeled versions (3K8u and 3K12u) of the peptides. This is particularly apparent for 3K8u, where NH–NH NOEs are not observed for the central residues of the peptide. We do not attempt to distinguish between populations of α- and 3_{10}-helical conformers, as sufficient αN and $\alpha\beta$ NOEs are not available

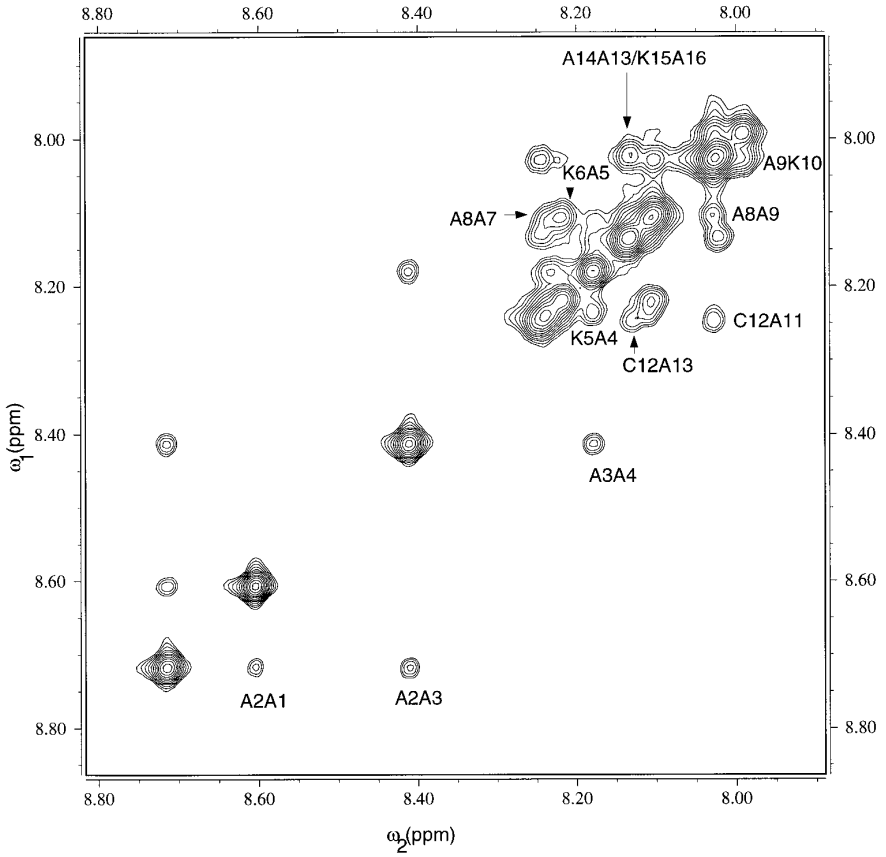

FIG. 3. NH−NH region of the 400-ms NOESY spectrum of N−O-reduced 3K12sl at pH 5 and 2°C. NN(i, i + 1) NOEs are labeled to show the assignments.

(*15*, *23*) and instead, analysis is confined to a comparison of the data for 3K8u, 3K8sl, 3K12u, and 3K12sl to the analogous data for 3K0.

Using the guidelines of Wishart and co-workers (*24*) and the recently calculated random coil shifts (δ_{rc}) for amino acids in peptides (*25*), the $C_\alpha H$ conformational shifts, where $\delta_{conf} = \delta_{expt} - \delta_{rc}$, were calculated and are shown in Fig. 5. An upfield, or negative, conformational shift indicates helical structure and a downfield, or positive, conformational shift indicates the presence of β-sheet structure. Comparison of these conformational shifts highlights the overall helicity of each of the peptides. All of the conformational shifts are negative and those greater than −0.1 ppm are assigned as regions of helical structure. While there is a small amount of scatter in the data, the conformational shifts for the Cys-SL peptides (3K8sl and 3K12sl) and 3K0 (Fig. 5B) show the same trends, with the N-terminus, Lys5, and Lys10 consistently having the most negative shifts, and the C-terminus having conformational shifts slightly more negative than −0.1 ppm. The Cys-SL residues for 3K8sl and 3K12sl also show very negative conformational shifts, but this could result from using the Cys random coil shift rather than one specific to the Cys-SL residue. There are no clear indications of local perturbations in the conformational shifts near the Cys-SL residues and the conformational shifts for 3K12sl are not systematically greater than those for 3K8sl; thus the conformational shift does not support a more helical structure for 3K12sl as indicated by CD.

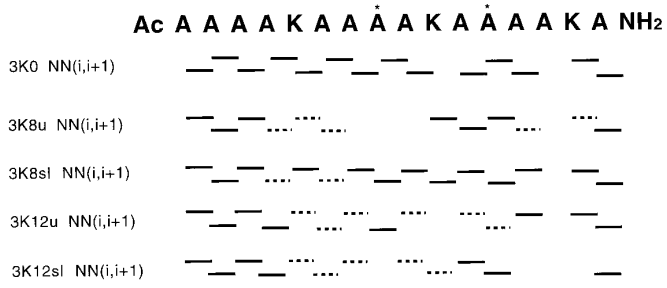

FIG. 4. NOE connectivity diagram indicating NN(i, i + 1) NOEs for each peptide. Dashed lines indicate partial overlap; completely overlapped NOEs are not shown. The asterisks indicate positions for the Cys-SL residue.

The unlabeled Cys peptides, 3K8u and 3K12u, are characterized by less negative shifts with four residues in 3K8u and six residues in 3K12u having conformational shifts less

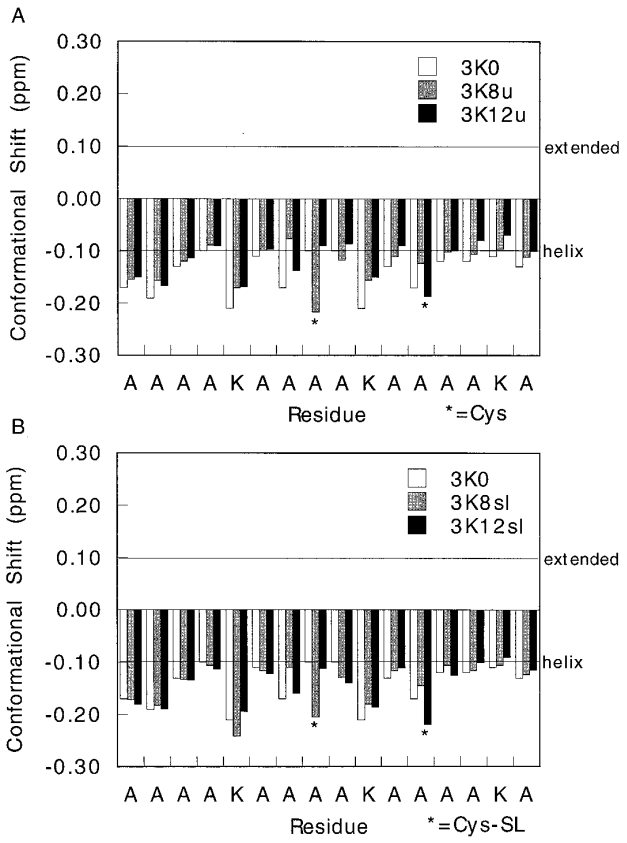

FIG. 5. Conformational shifts for 3K0 and (A) 3K8u and 3K12u and (B) N–O-reduced 3K8sl and 3K12sl (where $\delta_{conf} = \delta_{expt} - \delta_{rc}$). The uniformity of the conformational shifts in (B) suggests that the Cys-SL side chain does not perturb local helix structure.

negative than −0.1 ppm (Fig. 5A). However, the unlabeled peptides follow the same general pattern as the labeled peptides and 3K0, with more negative shifts observed at the N-terminus and center of the peptide and a decrease in conformational shift for the C-terminal four residues. These results are consistent with previous observations by NMR (*16*) and ESR (*4*) which report the most helical structure to be toward the center of the peptide. Aside from the large upfield conformational shifts of the Cys residues, there do not appear to be any distinct local perturbations, but rather a global loss of helicity resulting from the introduction of Cys into the sequence, which is consistent with the general shape of the CD curve and the 222 nm/208 nm ratios for the 3K8u and 3K12u peptides.

$^3J_{NH\alpha}$ coupling constants are directly related to the torsion angle ϕ according to the Karplus relationship (*26*). If a single conformer is present, it is possible to calculate ϕ from the measured coupling constant. However, for linear peptides in solution, rapidly sampling an ensemble of conformations, the resulting $^3J_{NH\alpha}$ is an average reflecting the populations of all ϕ angles sampled. Despite the averaged nature of the coupling constants, these data can be taken as a residue-specific indication of the extent of helical structures when comparing a series of closely related peptides, as any additional increase in coil population would lead to an increase in the magnitude of $^3J_{NH\alpha}$. While $C_\alpha H$ overlap precludes extensive analysis of the NOEs, the NH chemical shift dispersion makes possible the measurement of approximately 75% of the $^3J_{NH\alpha}$. The measured $^3J_{NH\alpha}$ are significantly smaller in magnitude than their corresponding per residue random coil values (*27*) and for the majority of residues in all of the peptides (>80%) $^3J_{NH\alpha} \leq 6$ Hz are observed (Fig. 6), indicating highly helical structures.

The $^3J_{NH\alpha}$ for the 3K8u and 3K12u peptides are, on average, greater than those for 3K8sl, 3K12sl, and the original 3K0 peptide, indicating a greater population of nonhelical conformers in the ensemble of conformers for the unlabeled peptides. However, a comparison of $^3J_{NH\alpha}$ for 3K8u and 3K12u reveals certain local differences which are not clearly observed in NOE or conformational shift analyses. In Fig. 6A it is apparent that the 3K8u peptide $^3J_{NH\alpha}$ are consistently

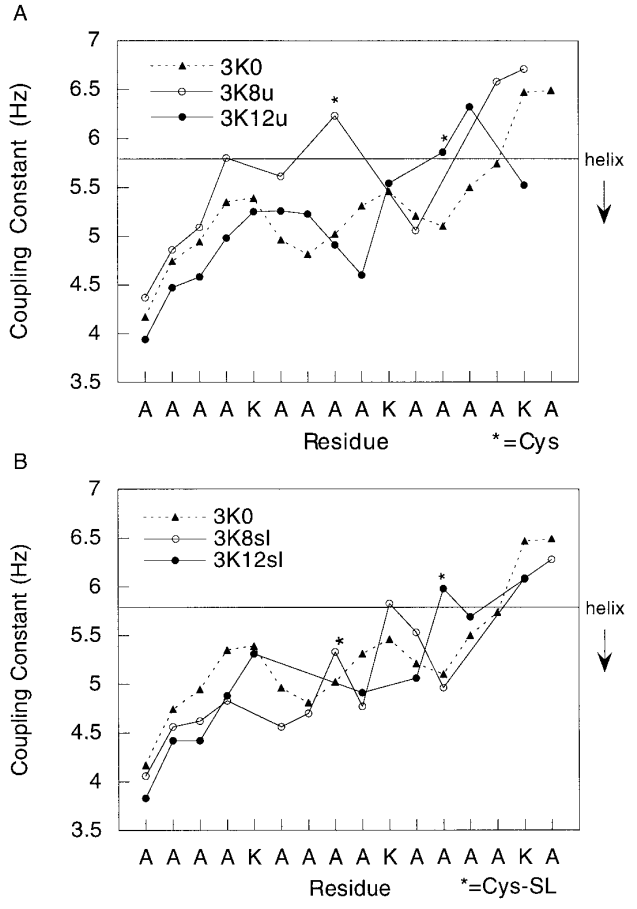

FIG. 6. Measured coupling constants ($^3J_{HN\alpha}$) for 3K0 and (A) 3K8u and 3K12u and (B) N–O-reduced 3K8sl and 3K12sl. To within experimental error, the position-dependent coupling constants for all the peptides in (B) are equivalent which suggests that the Cys-SL side chain does not perturb local helix structure.

greater than the corresponding $^3J_{NH\alpha}$ for the 3K0 peptide. In contrast, the 3K12u $^3J_{NH\alpha}$ for the N-terminal half of the peptide are nearly superimposable, within experimental error, with the 3K0 values. Only in the residues neighboring the free Cys do the 3K12u $^3J_{NH\alpha}$ diverge from the pattern of the 3K0 coupling constants.

Upon spin labeling, the $^3J_{NH\alpha}$ for 3K8sl decrease in magnitude until they overlap with the 3K0 values (Fig. 6B). The same effect is observed for the C-terminal half of 3K12sl. The $^3J_{NH\alpha}$ in the region of the Cys-SL residue decrease in magnitude such that there is overlap with the $^3J_{NH\alpha}$ for both 3K0 and 3K8sl. The 3K12u and 3K12sl $^3J_{NH\alpha}$ in the N-terminal half of the peptide are superimposable. Though there is some scatter between the $^3J_{NH\alpha}$ for the Cys-SL peptides and the values for the 3K0 peptide, they are the same within experimental error which is estimated to be approximately ± 0.3 Hz.

The differences between the free Cys and Cys-SL peptides seem to indicate that there are indeed perturbations by the free Cys which reduce local helicity and are dependent upon the position of the Cys residue. The effect of the helix-breaking Cys also appears to be greatest at the central position as in 3K8u. Both of these results are consistent with the trend observed by Baldwin and co-workers (*21*) when CD was used to study a series of 3K peptides with the helix-breaking residue Gly at different positions.

CONCLUSIONS

Analysis of the NMR data for this series of peptides, particularly the $^3J_{NH\alpha}$ coupling constants, confirms that while the introduction of a Cys residue into a highly helical model peptide destabilizes the helical secondary structure, the addition of the nitroxide spin label MTSSL to the Cys side-chain moiety restores global helicity, typical of the helix-supporting nature of unbranched aliphatic side chains. In addition, within the experimental error achievable for the coupling constants, there are no discernible local perturbations to the helical structure resulting from the spin labels when the Cys-SL peptides are compared to the 3K0 control peptide. From these results it must be concluded that Cys-SL is helix supporting similar to other unbranched aliphatic residues such as Met, Leu, and Ala. These results are consistent with the those of Hubbell and co-workers (*13*) from their extensive site-directed spin labeling studies of T4 lysozyme, in which substitution of solvent-exposed helical residues by the Cys-SL residue showed negligible change in biological activity and stability, and no change in secondary structure as monitored by CD.

REFERENCES

1. L. J. Berliner, J. Grunwald, H. O. Hankovszky, and K. Hideg, *Anal. Biochem.* **119,** 450 (1982).
2. G. L. Millhauser, *Trends Biochem. Sci.* **17,** 448 (1992).
3. W. L. Hubbell and C. Altenbach, *Curr. Opin. Struct. Biol.* **4,** 566 (1994).
4. S. M. Miick, K. M. Casteel, and G. L. Millhauser, *Biochemistry* **32,** 8014 (1993).
5. W. R. Fiori, S. M. Miick, and G. L. Millhauser, *Biochemistry* **32,** 11957 (1993).
6. W. R. Fiori, K. M. Lundberg, and G. L. Millhauser, *Nat. Struct. Biol.* **1,** 374 (1994).
7. M. Barranger-Mathys and D. S. Cafiso, *Biochemistry* **35,** 498 (1996).
8. C. Altenbach, S. L. Flitsch, H. G. Khorana, and W. L. Hubbell, *Biochemistry* **28,** 7806 (1989).
9. J. Voss, H. M. M., W. L. Hubbell, and H. R. Kaback, *Biochemistry* **35,** 12915 (1996).
10. M. D. Rabenstein and Y.-K. Shin, *Proc. Natl. Acad. Sci. USA* **92,** 8239 (1995).
11. C. L. North, J. C. Franklin, R. G. Bryant, and D. S. Cafiso, *Biophys. J.* **67,** 1861 (1994).
12. H. S. Mchaourab, K. J. Oh, C. J. Fang, and W. L. Hubbell, *Biochemistry* **36,** 307 (1997).
13. H. S. Mchaourab, M. A. Lietzow, K. Hideg, and W. L. Hubbell, *Biochemistry* **35,** 7692 (1996).
14. S. Marqusee, V. H. Robbins, and R. L. Baldwin, *Proc. Natl. Acad. Sci. USA* **86,** 5286 (1989).
15. G. L. Millhauser, C. J. Stenland, P. Hanson, K. A. Bolin, and F. J. M. v. d. Ven, *J. Mol. Biol.* **267,** 963 (1997).
16. G. L. Millhauser, C. J. Stenland, K. A. Bolin, and F. J. M. v. d. Ven, *J. Biol. NMR* **7,** 331 (1996).
17. C. Bartels, T. Xia, M. Billeter, P. Güntert, and K. Wüthrich, *J. Biol. NMR* **5,** 1 (1995).
18. T. Szyperski, P. Güntert, G. Otting, and K. Wüthrich, *J. Magn. Reson.* **99,** 552 (1992).
19. A. P. Todd and G. M. Millhauser, *Biochemistry* **30,** 5515 (1991).
20. N. R. Kallenbach, ''Circular Dichroism and the Conformational Analysis of Biomolecules'' (G. D. Fasman, Ed.), Chap. 7, Plenum Press, New York (1996).
21. A. Chakrabartty, J. A. Schellman, and R. L. Baldwin, *Nature (London)* **351,** 586 (1991).
22. C. Redfield, ''NMR of Macromolecules: A Practical Approach'' (G. K. C. Roberts, Ed.), p. 71, IRL Press, Oxford (1993).
23. S. M. Miick, G. V. Martinez, W. R. Fiori, A. P. Todd, and G. L. Millhauser, *Nature (London)* **359,** 653 (1992).
24. D. S. Wishart, B. D. Sykes, and F. M. Richards, *Biochemistry* **31,** 1647 (1992).
25. G. Merutka, H. J. Dyson, and P. E. Wright, *J. Biol. NMR* **5,** 14 (1995).
26. M. Karplus, *J. Chem. Phys.* **30,** 11 (1959).
27. L. J. Smith, K. A. Bolin, H. Schwalbe, M. W. MacArthur, J. M. Thornton, and C. M. Dobson, *J. Mol. Biol.* **255,** 494 (1996).